Run-up of Tsunamis by Linear and Nonlinear Theories

Chiaki Goto

Instructor of Civil Engineering
Tohoku University, Sendai, Japan

and

Nobuo Shuto

Professor of Civil Engineering
Tohoku University, Sendai, Japan

ABSTRACT

Linear and nonlinear sets of equations of long waves in the Lagrangian description are solved numerically to obtain run-up heights. Numerical results are compared with theoretical ones in case of simple topographies and the agreement is quite satisfactory. As a practical application, the computation is carried out for the Okkirai Bay in Japan. The computed run-up heighs agree fairly well with the recorded ones.

1. INTRODUCTION

One of the most difficult problems in the numerical simulation of tsunami run-ups lies in the fact that it is not easy to introduce the boundary condition which should precisely reflect the topography of the land where the tsunami arrives at.

In the present paper, one- and two-dimensional problems are treated numerically by adopting both linear and nonlinear sets of equations described in the Lagrangian coordinates. In this system, the boundary condition can be easily satisfied. The water particles lying on the sea bottom at the beginning of the motion do not leave the bottom during the subsequent motion. The water particle at the wave front is the one which is at the shoreline at the initial instant.

For the analysis, an explicit finite difference method is used. The computation is first carried out for simple topographies, for which the linear equation gives analytical solutions. The numerical results of the linear theory are compared with the theoretical values and agreement is quite satisfactory.

Then, the nonlinear computation is carried out. The difference between linear and nonlinear theories amounts 20% at most.

As an example of practical application, The computation is carried out for the Okkirai Bay on the South Sanriku Coast in Japan, which suffered much by the attacks of tsunamis in the past.

2. BASIC EQUATIONS AND NUMERICAL TECHNIQUES

Let us consider the irrotational, three-dimensional motion of an incompressible fluid. The displacements of the water particle which is at the point (a,b,c) at the initial instant is (a+x,b+y,c+z) at the time t. The still water surface is taken as the a-b plane, and the c-axis is taken vertically positive upward. Linear and nonlinear equations of long waves in the Lagrangian coordinates have been derived by authors (Shuto, 1967; Goto, 1979; Goto and Shuto, 1979).

The linear theory is written:

$$\eta + h(a,b)\{x_a + y_b\} + h(a+x,b+y) - h(a,b) = 0 \quad \text{---------(1)}$$

$$\begin{bmatrix} x_{tt} \\ y_{tt} \end{bmatrix} + g \begin{bmatrix} \eta_a \\ \eta_b \end{bmatrix} = 0 \quad \text{-----------(2)}$$

And the nonlinear one is

$$(1 + x_a + y_b)\{\eta + h(a+x,b+y) - h(a,b)\}$$
$$-h(a,b)\{x_a + y_b + \frac{\partial(x,y)}{\partial(a,b)}\} = 0 \quad \text{----------(3)}$$

$$\begin{bmatrix} 1 + x_a & y_a \\ x_b & 1 + y_b \end{bmatrix} \begin{bmatrix} x_{tt} \\ y_{tt} \end{bmatrix} + g \begin{bmatrix} \eta_a \\ \eta_b \end{bmatrix} = 0 \quad \text{------------(4)}$$

where g denotes the acceleration of gravity, h(a,b) the still water depth where the water particle existed at the initial instant and h(a+x,b+y) also still water depth where the water particle arrives at. The relationships between these theory is similar to that between linear long wave and shallow water theories in the Eulerian coordinates.

These equations are expressed in terms of the displacements (x,y,η) of the free surface from the original position. In the present analysis, the Lagrangian velocities $(u=x_t, v=y_t, \eta_t)$ are introduced in place of them. The bottom friction expressed in Manning's n and proportional to the square of the velocity is also introdeced. This change of variables makes the numerical computation more stable and easier.

Therefore, the equations are, for linear waves,

$$(\eta_t + uh_{a+x} + vh_{b+y}) + h(a,b)(u_a + v_b) = 0 \quad \text{----------(5)}$$

$$\begin{bmatrix} u_t \\ v_t \end{bmatrix} + g\begin{bmatrix} \eta_b \\ \eta_b \end{bmatrix} + \frac{gn^2}{D^{4/3}}\sqrt{u^2 + v^2}\begin{bmatrix} u \\ v \end{bmatrix} = 0 \quad \text{------------(6)}$$

and, for nonlinear waves,

$$(1 + x_a + y_b)^2(\eta_t + uh_{a+x} + vh_{b+y})$$

$$h(a,b)\{u_a + v_b + \frac{\partial(u,y)}{\partial(a,b)} + \frac{\partial(x,v)}{\partial(a,b)} = 0, \quad \text{----------(7)}$$

$$\begin{bmatrix} 1 + x_a & y_a \\ x_b & 1 + y_b \end{bmatrix}\begin{bmatrix} u_{tt} \\ v_{tt} \end{bmatrix} + g\begin{bmatrix} \eta_a \\ \eta_b \end{bmatrix} + \frac{gn^2}{D^{4/3}}\sqrt{u^2 + v^2}\begin{bmatrix} u \\ v \end{bmatrix} = 0 \quad \text{--------(8)}$$

Where D denotes the total water depth.

For the water particle at the initial instant, the still water depth h is equal to zero. Therefore, in these equations of continuity of long waves, the value $(\eta_t + uh_{a+x} + vh_{b+y})$ is equal to zero provides the boundary condition at the wave front.

For the numerical computation, an explicit finite difference method similar to the staggered leap-frog scheme is used. For example, the difference equations of the linear theory are expressed as

$$\eta^{n+1}_{i,j} = \eta^{n}_{i,j} - h_{i,j}\lambda\{(u^{n+1/2}_{i+1/2,j} - u^{n+1/2}_{i-1/2,j}) + (v^{n+1/2}_{i,j+1/2} - v^{n+1/2}_{i,j-1/2})\}$$

$$- \Delta t(h_x u^n_{i,j} + h_y v^n_{i,j}) \quad \text{----------(9)}$$

$$u^{n+1/2}_{i+1/2,j} = \frac{1}{1 + \mu^{n-1/2}_{i+1/2,j}}\{(1 - \mu^{n-1/2}_{i+1/2,j})u^{n-1/2}_{i+1/2,j}$$

$$- g\lambda(\eta^n_{i+1,j} + \eta^n_{i,j})\} \quad \text{---------(10)}$$

$$v^{n+1/2}_{i,j+1/2} = \frac{1}{1 + \mu^{n-1/2}_{i,j+1/2}}\{(1 - \mu^{n-1/2}_{i,j+1/2})v^{n-1/2}_{i,j+1/2}$$

$$- g\lambda(\eta^n_{i,j+1} + \eta^n_{i,j})\} \quad \text{---------(11)}$$

where $\lambda = \Delta t/\Delta s$; Δs and Δt denote horizontal and time mesh size, respectively, and

$$\mu^n_{i,j} = \frac{gn^2\Delta t}{(D^n_{i,j})^{4/3}}\{(u^n_{i,j})^2+(v^n_{i,j})^2\}^{1/2}.$$

Notations h_x and h_y denote the local slopes, in the x- and y-direction where the water particle arrives at, so we calculate and store them beforehand.

In Fig. 1, the numerical computation mesh is shown. The velosity are calculated for the point where arrows are shown and vertical displacement at the point where black circles are shown. When we need the velocities for the points of the black circles, we estimate them by a linear interpolation. For the points along the initial shoreline, we estimate the velosities by a linear extraporation.

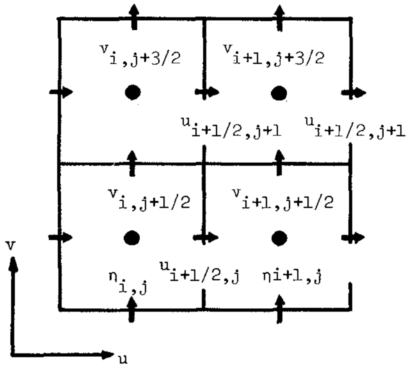

Fig. 1 Numerical mesh.

The same procedure was also adopted in case of nonlinear theory.

3. RESULTS OF COMPUTATION

(1) Comparisons with the analytical solutions.

First, we examine the accuracy of the numerical scheme for one-dimensional cases. A simple topography, a uniform slope connected to the channel of constant depth, is used. In this topography, the maximum run-up height R was theoretically presumed by Keller and Keller (1964) and confirmed by Shuto (1972), by using the linear theory.

$$\frac{R}{H} = \{J_0^2(4\pi\frac{l}{L}) + J_1^2(4\pi\frac{l}{L})\}^{-1/2} \qquad \text{----------(12)}$$

Where L is the wave length in water of constant depth, H the incident wave height, l the horizontal length between the toe of the slope and the shoreline and J_n the n-th Bessel Function of the first kind.

For the simple topography, we have computed several cases with no friction effect. Figure 2 shows the comparison. The curve is the result given by the analytical solution, while black circles are the numerical

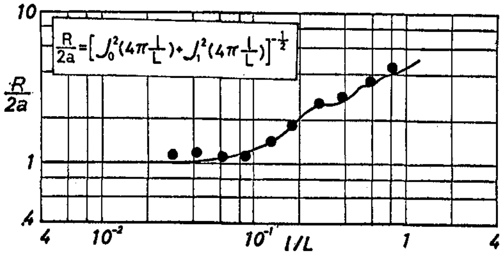

Fig. 2 The comparison between the analytical and the numerical (linear) results.

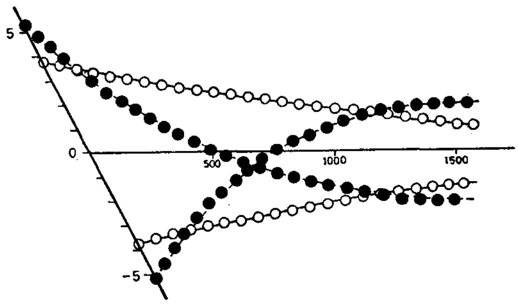

Fig. 3 The comparision of wave profile.

results. Examples of wave profile are shown in Fig. 3. They are for maximum run-up and run-down for wave periods of 300 sec and 600 sec by linear theory. The lines are the analytical solution and the circles the numerical results. We consider the agreement is satisfactory.

Though examination of the numerical results obtained for different conditions, we find that the accuracy of the numerical results depends upon three factors, the spatial mesh size Δs, the slope of topography α and the wave length L. In order to see this, the ratio of the computed maximum run-up height to the analytical one is shown in Fig. 4 as a function of a parameter made of the three factors. With the bigger value of the parameter, the accuracy becomes worse. The reason is considered due to deterioration of the linear extraporation used at the wave front, with steeper slopes, longer mesh size and shorter wave length.

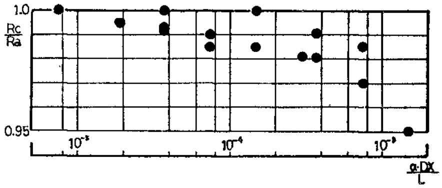

Fig. 4 The accuracy of the numerical computation.

Secondly, it is checked how big the effect of nonlinearity is. The computation is carried out for the same topography. The results are compared with analytical results of the linear theory. In nonlinear computations, a particle with the higher vertical displacement moves with the higher velocity. Therefore, in some cases, a particle behind the wave front overtakes the wave front. We consider that this introduces the breaking and it is necessary to make an adjustment. We set a restriction that the particles behind should not get ahead of the particles in front of them. White circles in Fig. 5 show the results of the computation with the adjustment and the black ones those without the adjustment. This phenomenon becomes distinct with the wave of big steepness. In the computation of actual tsunamis, the phenomena is almost negligible, because of their small steepness.

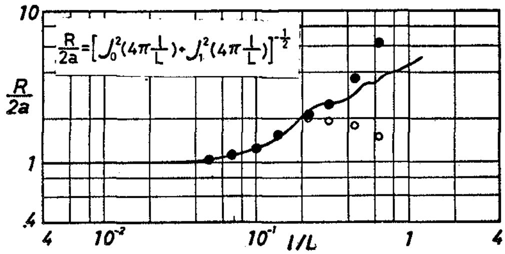

Fig. 5 The comparision between the analytical and the numerical (non-linear) results.

Examples of wave profile with the adjustment are shown in Fig. 6. The wave fronts are similar to a bore. However, due to the small amplitude, difference between the nonlinear results and the linear ones is not large.

Thirdly, the accuracy of our numerical scheme for the two-dimensional cases are examined. We employ the case of a rectangular bay with the bottom of a uniform slope. In this simple topography, an analytical solution of maximum run-up height are obtained by use of the linear theory in the Lagrangian coordinates as follows,

$$\frac{R}{H} = \{(J_1(4\pi\frac{l}{L})\psi_1)^2 + (J_0(4\pi\frac{l}{L}) - J_1(4\pi\frac{l}{L})\psi_2)^2\}^{-1/2}, \quad \text{------(13)}$$

where

$$\psi_1 = \frac{2kd}{\pi}\int_0^{kd} \frac{\sin^2 s}{s^2\sqrt{(kd)^2 - s^2}}\, ds,$$

$$\psi_2 = \frac{2kd}{\pi}\int_0^{kd} \frac{\sin^2 s}{s^2\sqrt{s^2 - (kd)^2}}\, ds,$$

and where 2d denotes the width of the bay and k the wave number. Tsunami in a bay may increase their heights due to resonance, and then the effects of nonlinearity may become unnegligible. Figure 7 shows the comparison of the analytical results of the linear theory and the numerical results. White circles are of nonlinear theory and black circles are of linear theory.

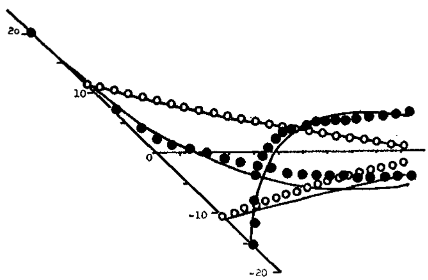

Fig. 6 Examples of wave profile for the nonlinear theory.

As the results of these preliminary examinations, we get the following conclusions.

1. Our numerical scheme is stable and satisfactory with respect to the accuracy of the results, for both one- and two-dimensional cases.

2. The nonlinear effects can increase the linear results by amount of 20% at most.

(2) An application to the Okkirai Bay.

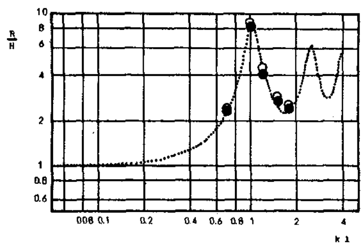

Fig. 7 The comparison between the analytical and the numerical results for a rectangular bay.

The method with the nonlinear and bottom friction (n = 0.029) effects is applied to a bay on the Sanriku Coast, in Japan. This area has been frequently attacked by tsunamis. In the Okkirai Bay, there are five fishing ports with flats behind them. Along the other part of the coast, we find the almost vertical cliffs and no village. Therefore, the main interests are upon the five places.

The tsunami selected as the input is the Great Meiji Sanriku Tsunami in 1896. Due to this tsunami, more than 27,000 persons were dead and about 10,000 houses were destroyed and lost. The source of the earthquake located at about 100km off the Sanriku Coast. Figure 8 shows the area of the source of the tsunami and the movement of the sea bottom which estimated by Hatori (1976). The number in the figure is the vertical displacement of the sea bottom. We assume that the displacement occured instantly and the water surface showed the same movements as the sea bottom.

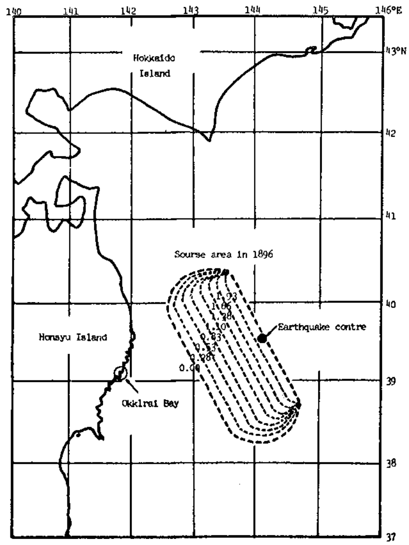

Fig. 8 The area of the source of the Tsunami in 1896.

In order to economize the computation time, the whole region is devided into four sub-regions of different mesh size. The minimum mesh size is 1/9km. Figure 9 shows the smallest region in the Okkirai Bay.

The origin of time is taken at the time when the earthquake occured. At about 17 minutes after the earthquake, the water level begins to recede. Then, it follows a slight ebb of water level. Figure 10 shows the time history of water surface elevation at the entrance of the bay.

An example of the numerical results is given in Figs. 11 to 15. In Figs. 11 and 12, which correspond to the time 2100 s and 2280 s, arrows show the horizontal velosities, lines the contour lines of the water surface and numbers attached the height in meters above still water level. Then, the first maximum run-up occurres at the bottom of the bay. We show the details in Figs. 13 to 15. The solid line is the network connecting the initial positions of water particles when we have no tsunami. The dotted line denotes the deformation of the network at each time. The

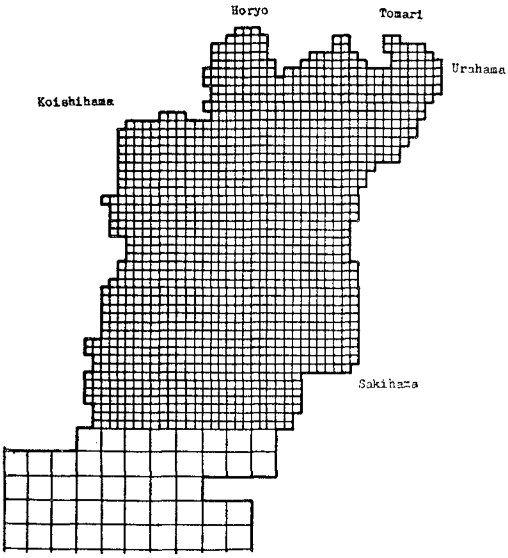

Fig. 9 The region of the smallest mesh in the numerical simulation.

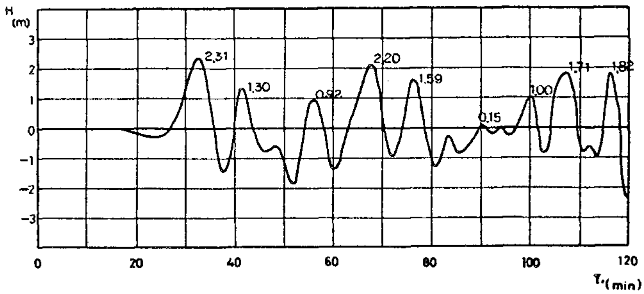

Fig. 10 The water level at the entrance of the bay.

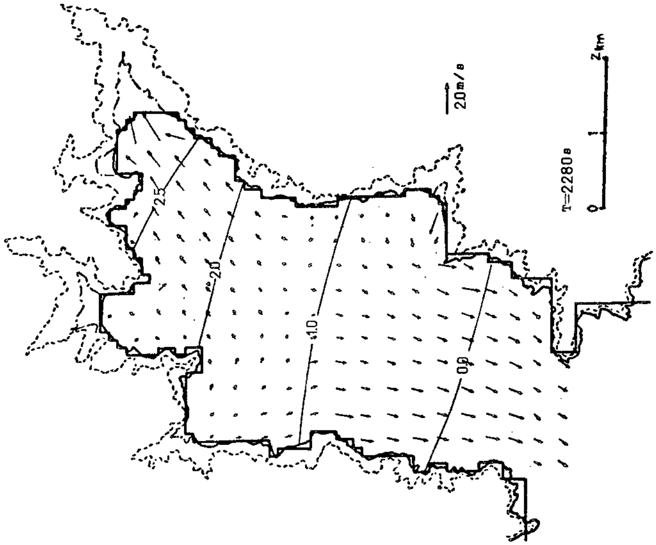

Fig. 12

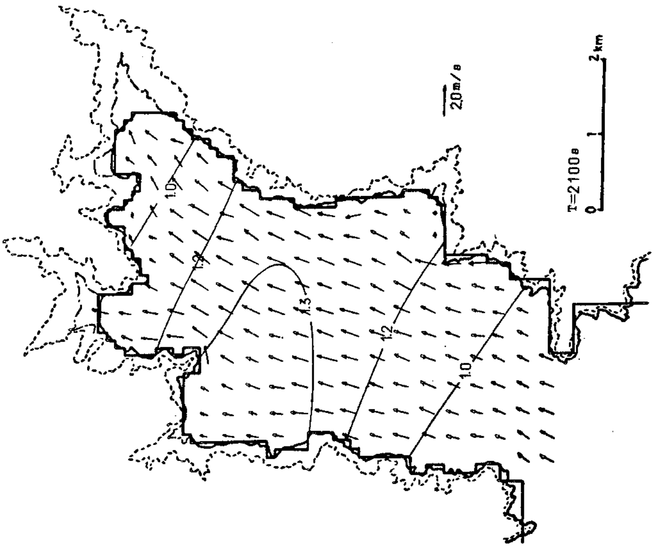

Fig. 11

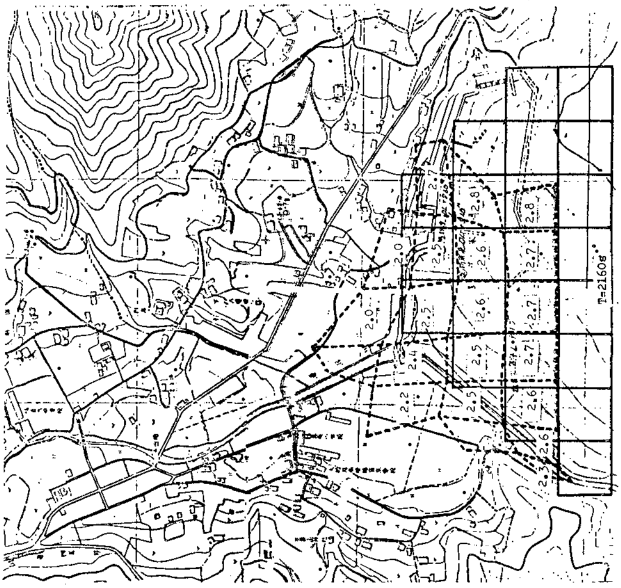

Fig. 14

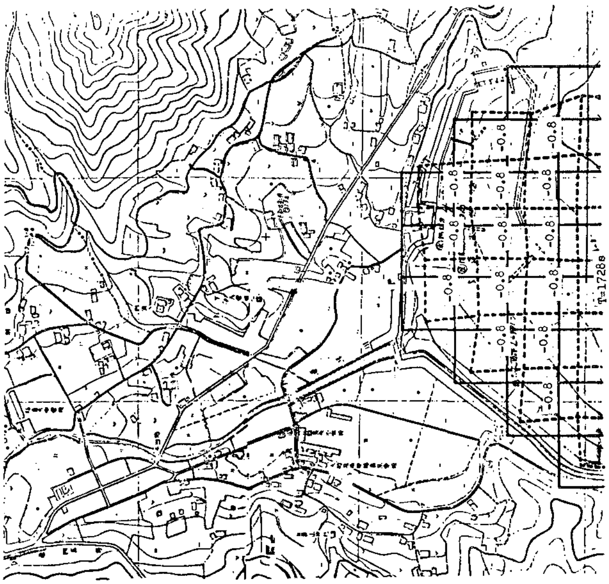

Fig. 13

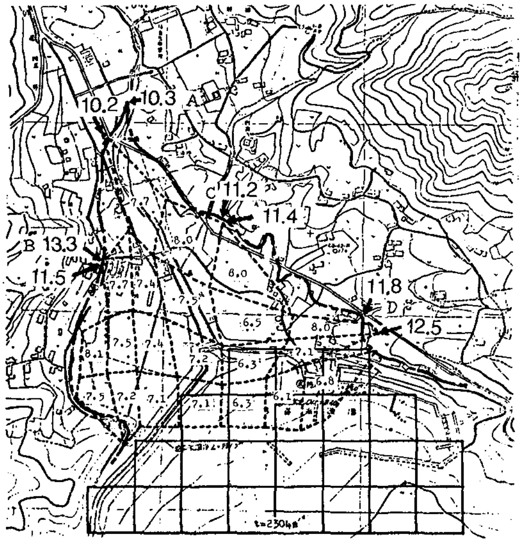

Fig. 15 The comparison between the recorded and the numerical maximum run-up height for the Great Meiji Sanriku Tsunami in 1896.

values shown in the center of the dotted mesh is the mean value of the vertical displacement, averaged from the value at four corners.

Figure 15 corresponds to the maximum run-up. The chain line in this figure shows the recorded inundation heights in 1896. There is a small river in this village. The record shows the run-up height of 10.3 m along the river (point A). The numerical simulation gives 10.2 m. Due to the finite grid cell, the computed point can not exactly coincide with the recorded point. At the point B, the record shows 13.3 m. The numerical ones is 11.5 m. Although the difference is rather big, the inundation lines of the recorded and the numerical ones coincide well, because the land here is almost vertical. At the point C, the record is 11.2 m and the computed one is 11.4 m. At the point D, 11.8 m and 12.5 m, respectively.

As the result, it is considered that the agreement is satisfactory and the method employed here is effective to simulate the run-up of a tsunami.

4. CONCLUSION

Linear and nonlinear long wave theories in the Lagrangian description are proved to be applicable to the analysis of tsunami run-up. Computation schemes are examined and established in both one- and two-dimensional cases. The present method can be also applied without difficulty to the actual topography of complicated geometry.

ACKNOWLEDGEMENT

The authors withed to express their gratitude to Dr. T. Iwasaki and Dr. A. Mano, Professors of Civil Engineering, Tohoku University, for their discussions and co-operation .

A part of the study was supported by a grant from the Ministry of Education.

REFERENCES

1) Shuto, N. : Run-up of long waves on a sloping beach, Coastal Engineering in Japan, Vol. 10, pp. 23-38, 1967.
2) Goto, C. : Nonlinear equation of long waves in the Lagrangian description, Coastal Engineering in Japan, Vol. 22, pp. 1-9, 1980.
3) Goto, C. and N. Shuto : Two-dimensional run-up of tsunami bynonlinear theory, Proc. of the 26th Conf. on Coastal Engineering in Japan,Vol. 26, pp56-60, 1979(In Japanese).
4) Keller J. B. and H. B. Keller : Water wave run-up on a beach, Research Report No. NONR-3828(00), Office of Navel Reasearch, Dept. of Navy, 1964.
5) Hatori, T. : Tsunami magnitude and wave source regions of historical Sanriku Tsunamis in Northest Japan, Bull. Earthq. Res. Inst. of Tokyo, University, Vol. 51, pp. 197-207, 1976 (In Japanese).